Article type: Full Paper

Dopant-Dependent Increase in Seebeck Coefficient and Electrical Conductivity in Blended Polymers with Offset Carrier Energies

Hui Li, Evan Plunkett, Zhengxu Cai, Botong Qiu, Tianran Wei, Hongyi Chen, Susanna M. Thon, Daniel H. Reich, Lidong Chen and Howard E. Katz*

Dr. H. Li, Prof. H. E. Katz
Department of Materials Science and Engineering, Johns Hopkins University, 3400 North Charles Street, Baltimore, MD 21218, USA
E-mail: hekatz@jhu.edu
E. Plunkett, Prof. D. H. Reich
Department of Physics and Astronomy, Johns Hopkins University, 3400 North Charles Street, Baltimore, MD 21218, USA
Dr. Z. Cai
School of Materials Science and Engineering, Beijing Institute of Technology, 5 South Zhongguancun Street, Beijing, 100081, China
Dr. H. Li, Dr. T. Wei, H. Chen, Prof. L. Chen
State Key Laboratory of High Performance Ceramics and Superfine Microstructures, Shanghai Institute of Ceramics, Chinese Academy of Sciences, Shanghai 200050, China
B. Qiu, Prof. S. M. Thon
Department of Electrical and Computer Engineering, Johns Hopkins University, 3400 North Charles Street, Baltimore, MD 21218, USA

Keyword:
polymer semiconductor, thermoelectrics, blend, chemical doping, density of states

Abstract: The strong and counterproductive interrelationship of thermoelectric parameters remains a bottleneck to improving thermoelectric performance, especially in polymer-based materials. In this paper, we investigate a compositional range over which there is decoupling of the electrical conductivity and Seebeck coefficient, achieving increases in at least one of these two parameters while the other is maintained or slightly increased as well. This is done using an alkylthio-substituted polythiophene (PQTS12) as additive in poly(bisdodecylquaterthiophene) (PQT12) with tetrafluorotetracyanoquinodimethane (F4TCNQ) and nitrosyl tetrafluoroborate (NOBF4) as dopants. The power factor increased two orders of magnitude with the PQTS12 additive at constant doping level. Using a second pair of polymers, poly(2,5-bis(3-dodecylthiophen-2-yl)thieno[3,2-b]thiophene (PBTTTC12) and poly(2,5-bis(3-

dodecylthiothiophen-2-yl)thieno[3,2-b]thiophene, (PBTTTSC12), with higher mobilities, we also observe decoupling of the Seebeck coefficient and electrical conductivity, and achieve higher power factor. Distinguished from recently reported works, these two sets of polymers possess very closely offset carrier energy levels (0.05 ~ 0.07 eV), and the microstructure, assessed using grazing incidence X-ray scattering, and mobility evaluated in field-effect transistors, was not adversely affected by the blending. Experiments, calculations and simulations are consistent with the idea that blending and doping polymers with closely-spaced energy levels and compatible morphologies to promote carrier mobility favors increased power factors.

1. Introduction

Organic thermoelectric materials are promising for lightweight, environmentally friendly, large-area and flexible devices for interconversion between heat and electricity.[1-2] The potential of a material for thermoelectricity can be assessed by a dimensionless figure of merit ZT,[3] which is defined by the relationship $ZT = S^2\sigma T/\kappa$, where S is the Seebeck coefficient, σ is the electrical conductivity, T is the absolute temperature and κ is the thermal conductivity. Usually, the power factor formula $PF = S^2\sigma$ is used to compare the energy conversion capabilities among different materials. Chemical doping of conducting polymers is an effective way to obtain high σ by controlling proportion of oxidized or reduced subunits in the polymers.[4-5] However, the improvement of the power factor is limited due to the interrelated and coupled parameters S and σ. In principle, S and σ are strongly and oppositely dependent on the carrier concentration associated with the electronic structure of the materials,[6] and can follow unfavorable opposing trends, which impedes the improvement of the PF. For disordered systems, the expressions of S and σ are different depending on various transport models.[7] If the carriers (holes) are only transported in the valence band, S is given by[8-10]

$$S = \frac{k_B}{e}\left(\frac{E_F - E_T}{k_B T} + A\right) \qquad (1)$$

where k_B is the Boltzmann constant, e is the elementary charge, E_F is the Fermi level, and E_T is the transport level which is not a generally used term in standard treatments of inorganic semiconductors. E_T was set as a constant by Arkhipov and Baranovskiiy.[11-13] On the other hand, it was defined as the mean energy of conducting charge carriers, and thus not a constant, as reported by Crispin and Pipe, which is suitable for amorphous materials.[14-15] Recently, E_T was

defined as the transport edge by Kang and Snyder. This definition gives the provision that charge carriers with energy $E < E_T$ do not contribute to the conduction.[16-17] The definition of E_T seems not to be completely standardized, and may be inconsistent in some references.[15, 18-19] As discussed further in section 2.7, we employ the definition of E_T as the averaged energy of carriers weighted by their contribution to conductivity.[20-21] A in the Equation (1) is a constant accounting for the entropy of carriers distributed below E_T. Thus, the Seebeck coefficient can be controlled by adjusting the energy level difference ($E_F - E_T$).

The decoupling of thermoelectric parameters was first discussed and developed in inorganic systems.[22-23] For organic systems, Katz et al. reported the increase of σ while S stayed nearly constant or increased slightly with the increase of dopant concentration over a narrow range using poly(3-hexylthiothiophene) (P3HTT) as a minor additive in poly(3-hexylthiophene) (P3HT).[24] It was assumed that most of the current is carried in the bulk P3HT, and the small amount of P3HTT modified the density of states (DOS) distribution as a result of the difference between the ionization potentials of the two polymers. In retrospect, differences in the associations of the dopants with the polymers and dopant-induced increased interchain interactions may have also played a role in those observations. While the PF values were very low (10^{-3} μW K^{-2} m^{-1}), this was the first sign that increasing the asymmetry of the DOS can help to decouple S and σ. Kemerink et al. recently reported examples of increased S obtained in post-deposition-doped (surface-doped) blend polymers although the decoupling was not mentioned.[25] They proposed that S can be increased with increasing the highest occupied molecular orbital (HOMO) energy difference between the two blended polymers according to a simplified equation (1) given by $S = (E_F - E_T)/eT$. Finally, a higher S was also achieved in an n-doped organic semiconductor by adding a small fraction of n-type semiconductor with a lower lowest unoccupied molecular orbital (LUMO) level.[26] These works suggest that it is possible to modify the electronic structure of a doped polymer system by using a minority polymer as an additive in a majority (matrix) polymer and achieve a net improvement in thermoelectric parameters.

As distinguished from our previous work,[24] we now focus on the simultaneous improvement of the Seebeck coefficient and electrical conductivity in much more conductive doped blend polymers than we had studied before. The first two polymers studied here, poly (bisdodecyl-

quaterthiophene) and poly (bisdodecylthio-quaterthiophene) (PQT12 and PQTS12, respectively), have the same backbone structure and would be expected to have similar and mutually compatible packing morphologies in films that would allow miscibility; this may also have been true of P3HT and P3HTT from the previous work but was not shown to be the case, while in the present work we used grazing incidence x-ray scattering to establish the similarities in the pure and blend polymer morphologies *in their doped states, which is most relevant for thermoelectric studies and which has not been done before*. Unlike in our previous work, two dopants, tetrafluorotetracyanoquinodimethane (F4TCNQ) and nitrosonium tetrafluoroborate (NOBF4), with different configurations, polarities, and oxidant activities, were chosen to dope these polymers. We used field-effect mobility measurements to further characterize dopant effects on hole transport capability and connect our data to reported empirical relationships. *We show that morphological compatibility of the two polymers and proper dopant selection allows for at least one of S and σ to be increased while the other is maintained or additionally increased in solution-doped polymers* by the combined contributions of offset energy levels and improved intermolecular associations. The sulfur atoms in the side chains of PQTS12 result in a perturbation of the highest HOMO level compared with PQT12, which allows for a tiny difference of oxidation potentials between the polymers; PQTS12 possesses a slightly lower onset oxidation potential (0.40 V) than PQT12 (0.45 V),[27] making the difference in HOMO levels about 0.05 eV. In later discussion, we explain that this is a theoretically preferred value for increasing power factor. Note that the goal of this work is not to increase absolute power factor in a single material, which can only be done by increasing mobility or introducing energy filtering effects, but rather to show that for a material system with a defined mobility, power factor can increase by blending structurally related polymers.

Also new in this work, a second set of higher-mobility polymers with more rigidly planar conjugated subunits, PBTTTC12 (poly(2,5-bis(3-dodecylthiophen-2-yl)thieno[3,2-b]thiophene) and PBTTTSC12 (poly(2,5-bis(3-dodecylthiothiophen-2-yl)thieno[3,2-b]thiophene), were synthesized and also showed a slight HOMO-level difference (0.07 eV) near the theoretically preferred value. This work adds support to the theoretical indication that using polymers with higher mobilities leads to higher PF in blends.

2. Results and Discussion

2.1 Thermoelectric data of PQT12/PQTS12 blends.

Figure 1 shows the thermoelectric properties of F4TCNQ-doped PQT12 and F4TCNQ-doped blend polymers. (Chemical structures of all polymers and dopants are shown in Figure S1). Electrical conductivity and Seebeck coefficient were measured as described before.[28] All data are collected from 4-5 devices and the error bars represent uncertainty as standard deviation. Addition of 3% PQTS12 into PQT12-1%F4TCNQ or into PQT12-3%F4TCNQ decreases the conductivity and increases the Seebeck coefficient (Figure 1a, 1b). This opposite trend of the two parameters follows the common expectation for thermoelectric measurements. However, adding more PQTS12 did not further decrease the conductivity. It is observed that *5% PQTS12 gives a result that S and σ simultaneously increase compared with the PQT12-5% F4TCNQ system* (Figure 1c). Thus, PF is one order of magnitude higher than that of PQT12-5% F4TCNQ.

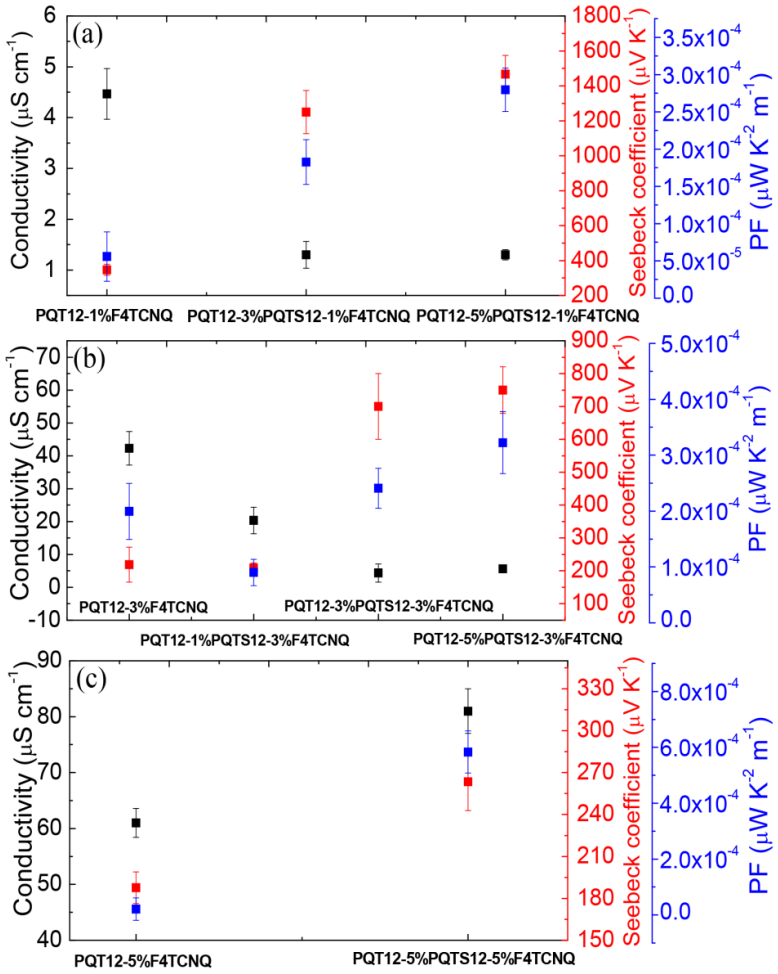

Figure 1. Thermoelectric properties of F4TCNQ-doped PQT12 and F4TCNQ-doped blend films.

The decoupling of *S* and σ was much more significantly observed using the stronger and more polar dopant NOBF4. As shown in Figure 2, the addition of PQTS12 into PQT12-NOBF4 systems results in generally simultaneous increases of *S* and σ, and the PF is significantly improved. The addition of 3% PQTS12 makes the PF 270 times higher than that of PQT12-1% NOBF4 (Figure 2a), and makes PF 7 times higher than that of PQT12-3% NOBF4, while 5% PQTS12 increases PF 50 times over the value for PQT12-3% NOBF4 (Figure 2b). Also, the addition of 5% PQTS12 makes PF 100 times higher than that of PQT12-5% NOBF4, mostly from increased *S,* while σ may have also increased somewhat (Figure 2c).

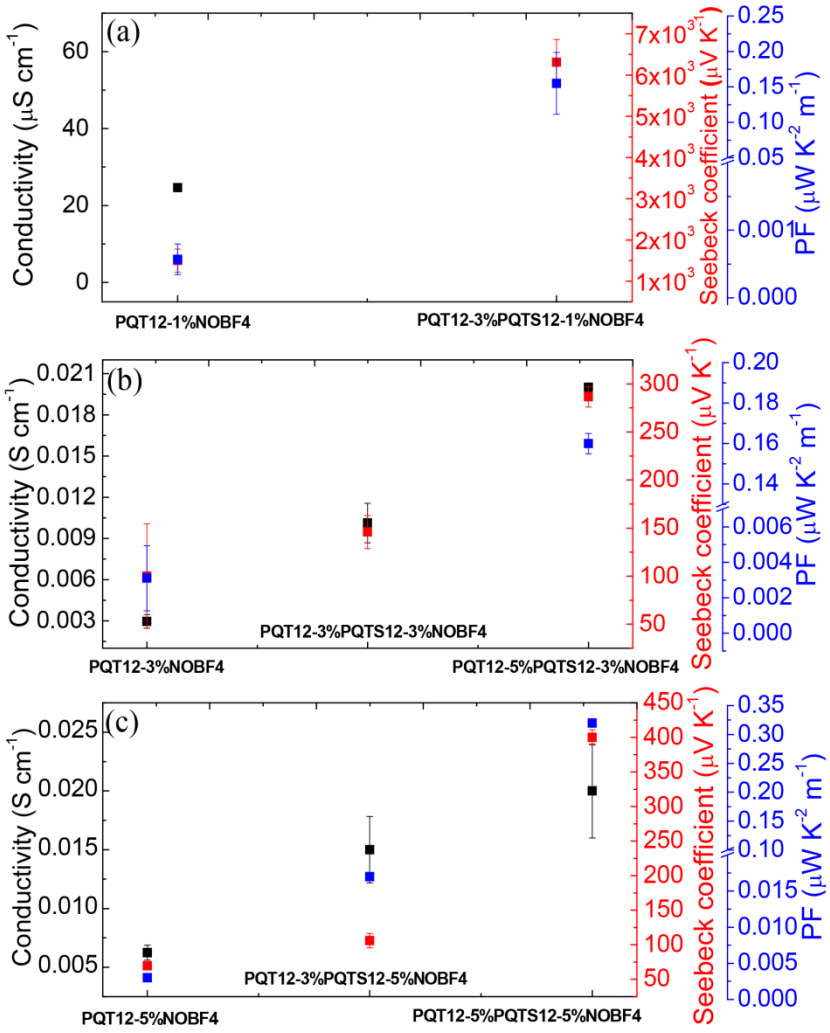

Figure 2. Thermoelectric properties of NOBF4-doped PQT12 and NOBF4-doped blend films.

2.2 Grazing Incidence X-ray Scattering.

As described above, both 3% PQTS12 and 5% PQTS12 can lead to simultaneously increasing *S* and σ while employing a constant dopant concentration. To check whether a microstructure difference from the addition of PQTS12 might be responsible, grazing incidence X-ray scattering (GIXRS) was employed to assess the crystallinity of pure polymer films and the blend polymer films. Only edge-on orientation can be observed in pure films. *Without dopant*, the scattering of PQTS12 itself was not observed after mixing 3% PQTS12 or 5% PQTS12 into PQT12 (Figure S2). However, the packing pattern of PQT12 was significantly changed in the blend film with 5% PQTS12 since both edge-on and face-on orientations appear, and the π-π stacking distance increases in the blend films (Table S1). That means the existence of PQTS12 contributes to disordering of PQT12 in blend films when 5% PQTS12 is added. However, the *doped blend films* show different packing behavior compared with the undoped blend films. The existence of 3% PQTS12 did not disturb the packing of F4TCNQ-doped PQT12 (Figure 3a, 3b) although the films were prepared by single-solution deposition instead of surface doping or vapor infiltration.[29] The lamellar structure and π-π stacking distance are almost the same as in PQT12-3%F4TCNQ (Figure S3). The addition of 5% PQTS12 slightly decreases the crystallinity of PQT12-3%F4TCNQ as the π-π stacking from doped-PQT12 (q_{xy} = 1.75 $Å^{-1}$) diminishes. The situation is different for the better-performing dopant NOBF4. For 3% NOBF4-doped film (Figure 3c, 3d and Figure S4), there is no change of lamellar structure or the π-π stacking distance with the addition of PQTS12, even for 5% PQTS12. That indicates PQTS12 did not alter the packing of NOBF4-doped PQT12. We note that the in-plane crystallinity (q_{xy} axis) of PQT12-3%F4TCNQ or PQT12-3%PQTS12-3%F4TCNQ is somewhat similar with the PBTTT-F4TCNQ system in which F4TCNQ and PBTTT-C14 order in a cofacial arrangement.[30] The scattering near q_{xy} = 1.5 $Å^{-1}$ (*d*-spacing of 4.18 Å) is assigned to the stacked conjugated backbones of the polymers, and the scattering at q_{xy} = 1.74 $Å^{-1}$ (*d*-spacing of 3.61 Å) can be attributed to the packed F4TCNQ-polymer crystallites. These two kinds of crystalline domains were not disturbed by adding 3% PQTS12. This suggests that F4TCNQ molecules preferentially interact with the PQT12 backbone rather than the PQTS12 backbone in the blend film. But the addition of 5% PQTS12 impedes the balance of these two packing structures and makes no contribution to the intensity of dopant-polymer domains. In NOBF4-doped films, only the scattering from the π-π conjugated backbones of polymers (q_{xy} = 1.5 $Å^{-1}$) was observed.

Although separate domains were not observed in the NOBF4-doped blend film, NOBF4 may be prone to dope PQTS12 preferentially because the sulfur group in the side chains could act as a binding site for NOBF4.[28] Considering that high conductivity and PF were obtained using NOBF4 in our previous work, NOBF4 seems to be a better choice for the power factor enhancement in the present work.

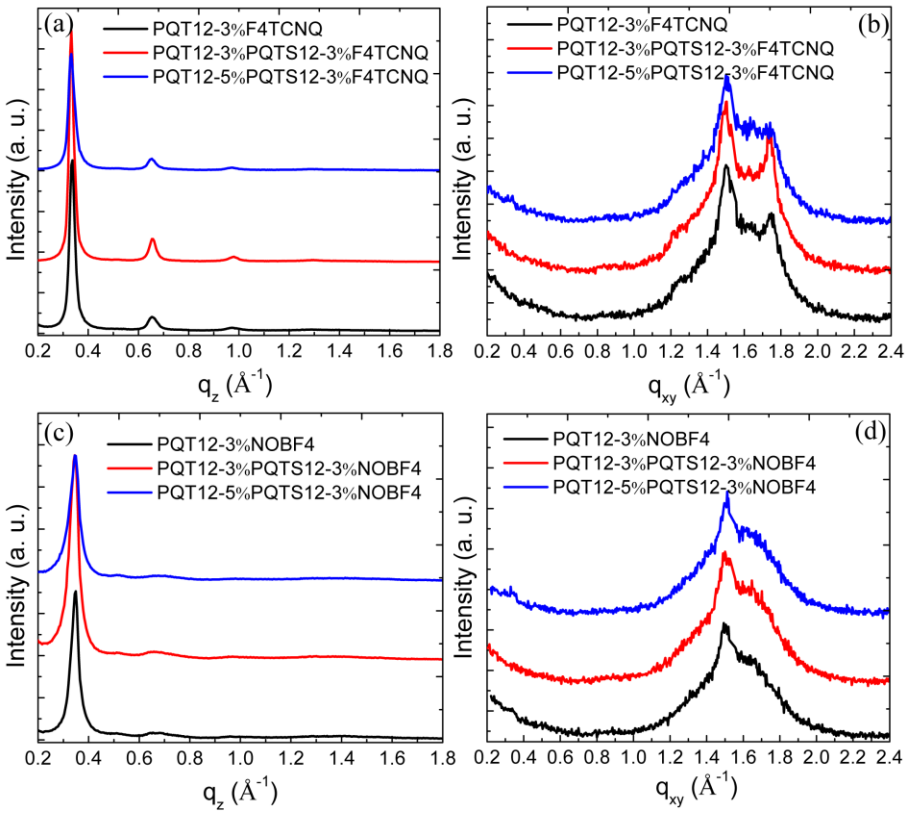

Figure 3. GIXRS line profiles of doped PQT12 and doped blend films. (a, c) Out-of-plane pattern; (b, d) In-plane pattern.

2.3 Electrochemical properties and doping levels of PQT12/PQTS12 blends.

The effects of additive polymers on the electrochemical properties and doping levels of blend films were investigated using cyclic voltammetry (CV) and UV-vis-NIR absorption measurements. For example, the addition of 3%PQTS12 cannot change the oxidizability of PQT12 (Figure S5) because of negligible PQTS12 content. The absorption spectra of doped films show low doping levels via the weak absorption intensity of the charge-transfer complex (700 ~ 2000 nm) compared with the intensity of the neutral polymer peak (400 ~ 700 nm) (Figure S6). This is predictable because only 0.02 ~ 0.2 (molar ratio) dopant molecule to one

repeat unit (four thiophenes) of PQT12 polymer was included. Because of the higher oxidizing activity of NOBF4 compared to F4TCNQ, NOBF4 gives a higher doping level than F4TCNQ when the same dopant concentration was used. We found the addition of PQTS12 slightly affects the doping level of the films.

2.4 PBTTT polymers with higher mobility.

Although the PF of the blend film is improved to 0.3 μW K^{-2} m^{-1}, two orders magnitude higher than the value in our previous work,[24] the thermoelectric performance of NOBF4-doped PQT12/PQTS12 blend is still lower compared with prior results on solution-doped single polymers. [31-32] Therefore, we synthesized polymers PBTTTC12 and PBTTTSC12 according to literature procedures.[28, 33] These are expected to be morphologically compatible but have higher mobility. The transfer and output curves of transistors based on the two polymers are shown in Figure S7 to illustrate the effect of blending on charge carrier mobility. The mobility is 0.13 cm^2 V^{-1} s^{-1} and 0.01 cm^2 V^{-1} s^{-1} for PBTTTC12 and PBTTTSC12, respectively. The HOMO level difference of the two polymers is 0.07 eV ($PBTTTC12_{HOMO}$ = 5.15 eV, $PBTTTSC12_{HOMO}$ = 5.08 eV) as determined by CV (Figure S8). Doped with F4TCNQ, only PBTTTC12-3%PBTTTSC12-3%F4TCNQ shows a simultaneous doubling of σ and 50% increase in S (Figure 4a). Although the decoupling of S and σ occurs at much lower doping levels, where morphological distortion of polymers by F4TCNQ is minimized, the PF value of this combination is higher than those of PQT12/PQTS12 blends. In particular, the conductivities of 3%NOBF4-doped blends are one order of magnitude higher than those of PQT12/PQTS12 blends, and the σ and S are significantly decoupled. Finally, the highest PF is 1.2 μW K^{-2} m^{-1} for the PBTTTC12-3%PBTTTSC12-3%NOBF4 film, where S nearly doubles while σ is at least maintained (Figure 4b), which is comparable to that of the solution-doped PBTTTC12.[32] This indicates that the high mobility of each polymer is crucial to improve the performance of blend systems. The 5% NOBF4-doped blend shows an increase of σ but the S starts out small because of the higher mobile charge carrier density and stays almost the same when more PBTTTSC12 is added (Figure 4c), so the PF does not increase.

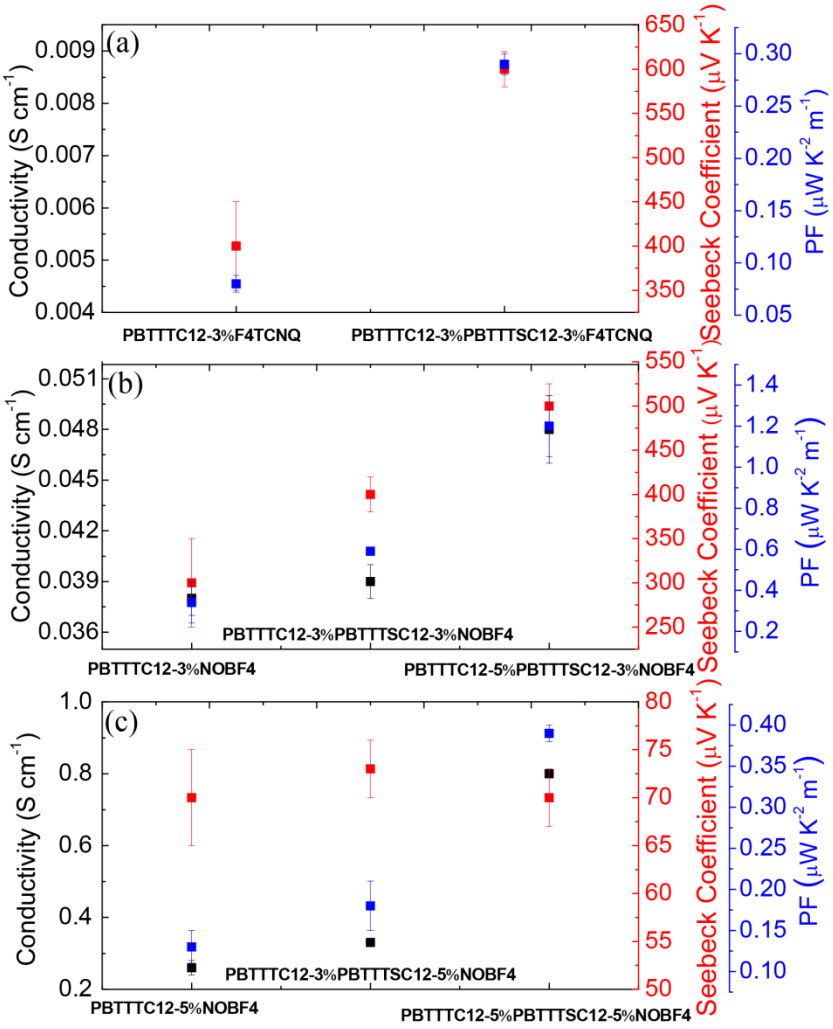

Figure 4. Thermoelectric properties of F4TCNQ-doped PBTTTC12 and F4TCNQ-doped blend films (a); NOBF4-doped PBTTTC12 and NOBF4-doped blend films (b, c).

2.5 Field-effect transistor characterization of blend polymers.

To further investigate the influence of alkylthio-substituted polymer on the electric properties of the blend films with dopants, we compared the mobility of NOBF4-doped single-polymer films with that of NOBF4-doped blend films. The illustrative set of transfer curves and output curves is shown in Figure 5, with other combinations shown in Figure S9. For films in which the conductivity is very low, the ohmic current can be ignored and the field-effect mobilities μ could be extracted from the linear regime. However, for conductive polymer films (NOBF4-doped PBTTTC12 film and NOBF4-doped blends), the drain current in output curves is carried by a parallel connection of the transistor channel and an ohmic current in the bulk that is not

influenced by the gate potential.[34] Therefore, the field-effect mobilities μ were extracted according to the more suitable equation as follows:

$$I_D = \mu \frac{W}{L} C_i \left[(V_G - V_T) - \frac{V_D}{2} \right] V_D + \frac{V_D}{R_{parallel}}, \ (V_G\text{-}V_T) \geq V_D \qquad (2)$$

where I_D is the source-drain current, W and L are channel width and channel length, respectively, C_i is the capacitance per unit area of the insulator, V_G and V_D are gate voltage and source-drain voltage, respectively, and V_T is the threshold voltage. $R_{parallel}$ is the parallel resistance that is determined by the electrical conductivity of the doped film. All data are summarized in Table S2. The mobility of single-polymer films or blend films increases with more dopants being added into the polymers because of the cancellation of traps. Furthermore, the mobilities of blend films with 3% alkylthio-substituted polymer slightly decrease compared with single-polymer films, while the addition of 5% thio-substituted polymer significantly improves the mobility of doped blend films. For instance, the mobility of PBTTTC12-5%PBTTTSC12-5%NOBF4 is 2.5 $cm^2\ V^{-1}\ s^{-1}$, which is 5 times higher than the mobility of PBTTTC12-5%NOBF4.

If it is assumed that all dopants become anions, the charge density in the bulk of the films is equivalent to the NOBF4 concentration, amounting to $10^{20}\ cm^{-3}$. The mobility is given by

$$\sigma = ne\mu \qquad (3)$$

where n is the carrier concentration and e is the elementary charge. The calculated mobility in this case is about one or two orders of magnitude smaller than the average value measured from field effect transistors. This indicates that the mobility of carriers in the bulk of the films, which includes mathematical contributions from all of the added carriers, is smaller than the mobility of carriers in the accumulation regime at the insulator-semiconductor interface. Therefore, we conclude that most of the carriers generated from charge transfer between the polymer and dopant at the low levels under consideration here are trapped, and the initially added dopants cannot contribute to the conductivity. However, such traps are more efficiently filled with much higher dopant concentrations in systems of highly conductive polymers.[28] The relationship between mobility and conductivity is shown in Figure S10. This relation is in good agreement with previously reported treatments, [34-35] which means both sets of data are fitted to a power law: $\mu \propto \sigma^{\delta}$, ($\delta \approx 0.7$). In our work, δ is between 0.65 and 0.71.

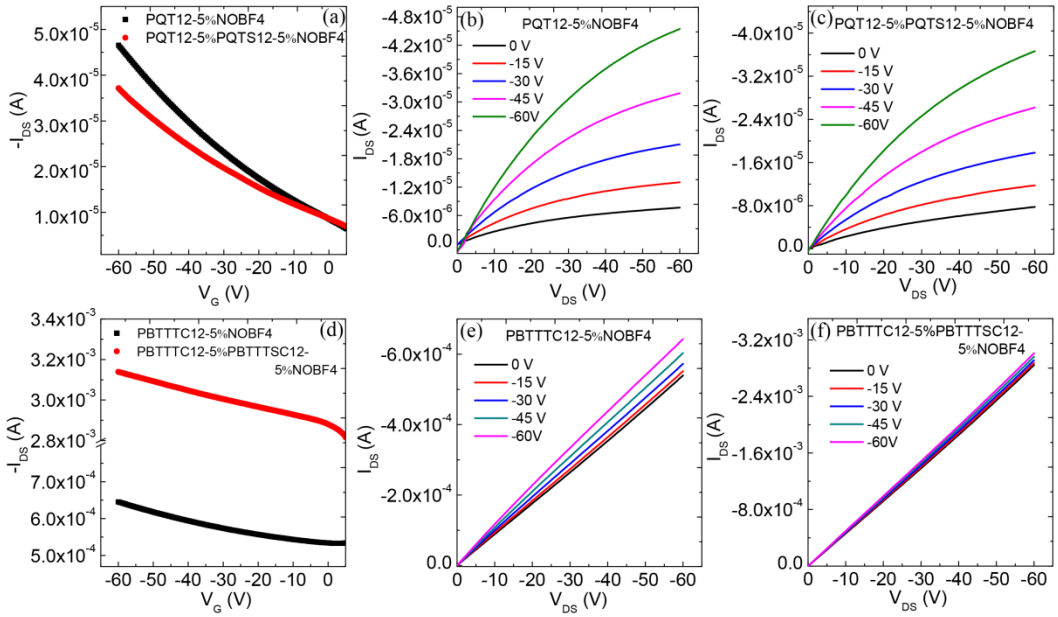

Figure 5. Transfer and output characteristics of OFETs based on 5%NOBF4-doped single polymer and 5%NOBF4 doped blend polymer. Transfer curves were measured with V_{DS} = -60 V.

The conductivities from OFETs were compared with Snyder's relationship[16] (Figure S11), where edge conductivities were associated with transistor conductivities just above the threshold voltages.[36] The charge density would be 0.01 C cm^{-3} estimated from our output curves assuming that a 5 V gate voltage is needed to turn on the NOBF4-doped PQT12 OFET device and NOBF4-doped PQT12/PQTS12 OFET device (the thickness of the polymer film is 50 nm and the gate oxide capacitance is 10 nF cm^{-2}). The mobility would be 0.003-0.03 cm^2 V^{-1} s^{-1} for the σ_{E0} interval between 3 × 10^{-5} and 3 × 10^{-4} S cm^{-1}. Our measured mobilities of doped blend films agree with this model (green and blue outlined pentagrams) except for the 1%NOBF4-doped films because of inefficient doping in those samples. For 3%NOBF4-PQT12 and 5%NOBF4-PQT12, our thermoelectric parameters are below the levels associated with σ_{E0} of 3 × 10^{-5} S $cm^{-1}s^{-1}$ (mobility 0.0003-0.003 cm^2/Vs, violet-blue and green dots), which can probably be attributed to the trap (localized) states above the transport states. If the same calculation is applied to 3%NOBF4-doped PBTTTC12 and its blends (purple dot and outlined pentagrams), the transistor mobility would also agree with the one determined from σ_{E0} and charge density). For %NOBF4-doped PBTTTC12 and its blends (dark pink dot), the gate voltage needed to turn on these OFET transistors is much smaller. If a 0.05 V gate voltage is needed to turn on these

transistors, the mobility would be 0.3 to 3 $cm^2\ V^{-1}\ s^{-1}$ for the σ_{E0} interval between 3×10^{-5} and 3×10^{-4} S cm^{-1}.

We also mapped these data onto the Chabynic relationship[32] (Figure S12). We found that the data of the PBTTTC12/PBTTTSC12 blends are located at regions where conductivity is in the high range for a given Seebeck coefficient. It should be noted that some data are above the line ($S \propto \sigma^{-1/4}$) for the relationship, because the empirical relationship data do not have the blending enhancements. This is further evidence for the blending strategy increasing the power factor above what is typically obtained for single polymers with comparable conductivities.

2.6 Possible mechanism for decoupling of electrical conductivity and Seebeck coefficient.

Because the dopant (F4TCNQ or NOBF4) was added after the two polymers were mixed, the doping occurs at random locations in the blend but thermodynamically prefers to extract electrons from the more easily oxidized polymer and/or the polymer with which it has the strongest nonbonded interactions. Using PQT12 (the majority component) and PQTS12 (an "additive"), in consideration of the results of GIXRS, F4TCNQ will prefer to interact with PQT12, and NOBF4 is prone to oxidize PQTS12. In addition, organic materials tend to have a high density of in-gap trap states resulting from energetic and structural disorder.[12, 37-39] Therefore, we propose that the blending of PQT12 and PQTS12 introduces deep trap states where holes are at lower energy (greater stability) than they are in the transport states. The energy-level diagram of doped films is shown in Figure 6. Transport of doping-induced carriers can be hindered by the deep trap states at very low doping concentration. Furthermore, the carriers would contribute to electrical conductivity only if they are activated to the transport level (close to the HOMO of PQT12) (Figure 6a, 6c). For F4TCNQ-doped blend films, the transport of carriers is dominated by F4TCNQ-PQT12 complexes. The addition of PQTS12 means more traps and lower doping efficiency for PQT12 in the blend film so that the conductivity decreases compared with F4TCNQ-doped PQT12 (Figures 1a-b). Meanwhile, the Fermi level of the blend film stays close to the HOMO of PQTS12 (Figure 6b).[24-25] This will result in an increase of E_F-E_T in the PQT12-PQTS12 blend film relative to PQT12 alone, and thus an increase of Seebeck coefficient. A further increase of the doping concentration leads to the generation of more free charge carriers. Ultimately, a simultaneous, modest increase of σ and S is observed in Figure 1c;

this unusual behavior of S and σ with increased PQTS12 additive may be attributed to an increased E_F - E_T as well as a possible increase in the number of carrier configurations around E_T of PQT12 as well as higher carrier mobility when PQTS12 and F4TCNQ are both present at 5% concentrations.

NOBF4-doped PQT12 shows a narrow gap between E_F and E_T (Figure 6c). For NOBF4-doped blend films, the addition of PQTS12 induces more free carriers in transport states because of the favored NOBF4-PQTS12 interaction, which is responsible for higher conductivity in blend films. Although a down-shift of the Fermi level (more holes induced) would occur for NOBF4-doped PQTS12, the Fermi level of the blend film is still at lower hole energy (closer to the LUMO) compared with NOBF4-doped PQT12 (Figure 6d), and there is a ΔE shift of the Fermi level between NOBF4-doped PQT12 and NOBF4-doped blend film. Thus, the difference ($E_F - E_T$) again increases in the blend films, resulting in an increased Seebeck coefficient.

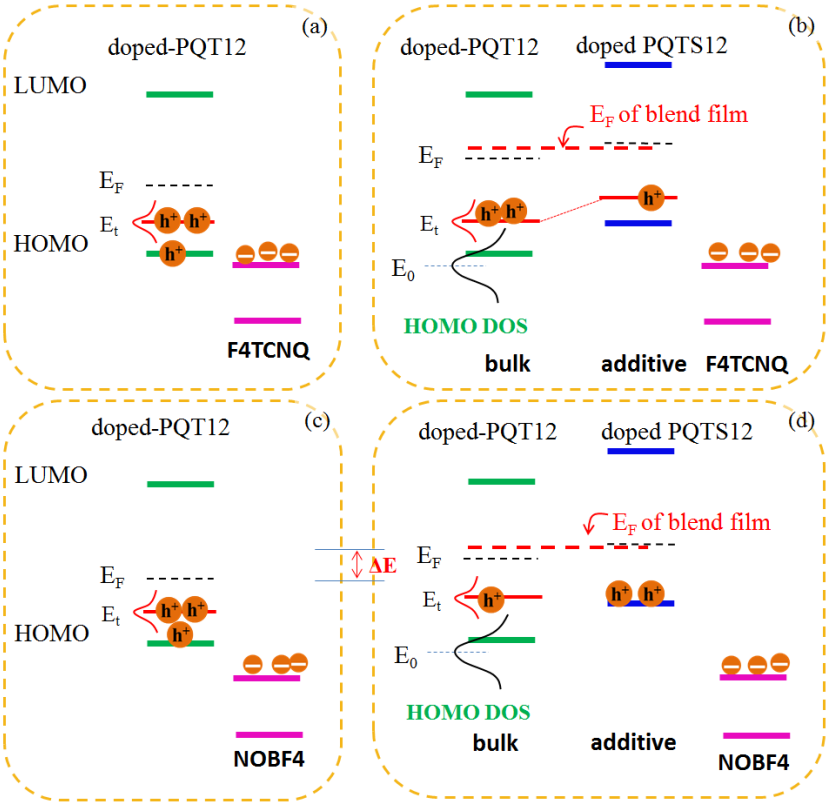

Figure 6. Schematic energy-level diagrams of doped PQT12 (a, c) and doped blend polymer films with two different dopants (b, d). Higher vertical positions indicate greater stability of holes.

2.7 Simulation model for high power factor.

In this work, the strategy to improve the PF value is blending two polymers with slightly offset HOMO levels to maintain the Seebeck coefficient when doping. It is of interest to determine the preferred HOMO energy difference for the highest PF in blend films. Since the additive polymer will define the Fermi level of blend films when the additive polymer is only partially ionized, the answer to this question can be focused on the preferred E_F - E_T in blend films. We note that the PF is related to S and σ. According to the Equation (3), $\sigma = ne\mu$, and n is related to the DOS and the Fermi-Dirac distribution function,[40] that is,

$$n = \int \frac{g(E)}{1+\exp(\frac{E-E_F}{k_BT})} dE \qquad (4)$$

where *g(E)* is the carrier DOS and is assumed to be the Gaussian distribution. *g(E)* can be described as

$$g(E) = \frac{N_t}{\sqrt{2\pi}\alpha} \exp(-\frac{E^2}{2\alpha^2}) \qquad (5)$$

where N_t is the number of states per unit volume, α is the energetic disorder and related to the material morphology, [14, 36, 41-42] and $\alpha_0 = \alpha/k_BT$ indicates the width of the DOS.[40]

Therefore, the PF can be given as

$$PF = a(\eta - \varepsilon_t + A)^2 \cdot \int \frac{\frac{b}{\alpha_0}\exp\left(-\frac{\varepsilon^2}{2\alpha_0^2}\right)}{1+\exp(\varepsilon-\eta)} d\varepsilon \qquad (6)$$

Where $\eta = E_F/k_BT$, $\varepsilon_t = E_T/k_BT$, $\varepsilon = E/k_BT$. The detailed calculation is shown in SI.

Here *a* and *b* are regarded as constant values for a certain system. The parameter *a* is related to the mobility. It is possible for the mobility to also be a function of energy *E*, but our experiments show that the mobility does not change much with low doping levels, so making mobility a constant is reasonable. Therefore, we can simulate the PF vs η curves according to the Equation (6), which are shown in Figure 7, and obtain the maximum PF value with the corresponding value of E_F-E_T.

We need to consider the effect of three parameters (A, α_0, and E_T) on the PF vs η curve in Equation (6). E_T is approximately the averaged energy of carriers weighted by their contribution to conductivity, and it would vary with doping. We will discuss the effect of variable E_T later, but first we chose E_T to be an arbitrary value for simplifying the description of A and α_0 as follows: (1) It is noted that A in Equation (6) reflects the details of the energy-dependent electrical conductivity and could be changeable according to the work of Cutler and Mott.[43] As described in Kemerink's work,[25, 44] the DOS distribution, and thus A, can be affected by blending or doping, and could be reasonable to be in the range of 0.5-1.5.[8] If it is defined that ε_t = 1 (E_T = 1 k_BT) and α_0 is a constant, Figure 7a is obtained with the varied A. We found that the E_F - E_T values for the range of A are all of the same order of magnitude and close to our experimental difference (0.06 ~ 0.09 eV); (2) The DOS distribution could be broadened with doping, so α_0 could be another changeable parameter in the Equation (6). If it is defined that ε_t = 1 (E_T = 1 k_BT) and A = 1, we can derive Figure 7b with varied α_0. It shows that the effect of different α_0 on the position of E_F/k_BT for maximum PF is negligible, which means the energetic disorder cannot change the E_F-E_T values; (3) Since the transport level E_T (ε_t) changes with doping, the absolute value of E_T will affect the position of maximum PF relative to E_F-E_T (Figure S13a), however, the E_F - E_T values (0.04 ~ 0.08 eV) are still close to our experimental difference. It is noted that the varying of E_T from 1 k_BT to 3 k_BT means the energy of conducting charge carriers and the conductivity distribution change with doping. For the curve A = 1, E_T = 1 k_BT in Figure S13a, we employ a mobility from Table S2, for example, 0.035 cm^2 V^{-1} s^{-1} for PQT12-5%PQTS12-5%NOBF4, and thus obtain the simulated PF values with varied α_0 (Figure S13b). The simulated PF value is close to the experimental PF of 0.32 μW K^{-2} m^{-1}, especially for low α_0. This is also applied to the PBTTTC12-5%PBTTTSC12-3%NOBF4. In this combination the simulated PF value is 1.25 μW K^{-2} m^{-1} at E_T-E_F = 0.07 eV (α_0 = 1.5) while the experimental average PF value is 1.2 μW K^{-2} m^{-1}.

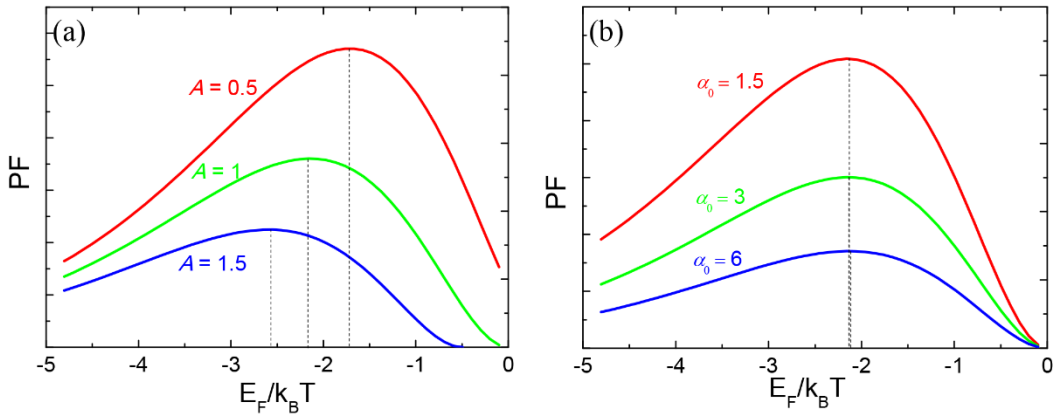

Figure 7. The simulated curves of Equation (6) with varied A (left: $\varepsilon_t = 1$, α_0 is constant) and varied α_0 (right: $\varepsilon_t = 1$, $A = 1$).

Furthermore, representative temperature dependences of σ and S were measured and plotted in Figure S14. The σ slightly increases with the temperature changing from 315 K to 348 K (70 ºC), and S is almost unchanged from 318 K to 345 K, which is consistent with the temperature-activated transport.[15, 45-47] This occurs both in PQT12-3%NOBF4 and PQT12-5%PQTS12-3%NOBF4, indicating that these two measurements are related correctly. Dedoping and/or degradation occur above 348 K since σ decreases significantly and S increases, simultaneously, which is common in polythiophenes.[48-49] The transport activation energy (E_A) calculated from σ versus T plots is 0.068 eV and 0.088 eV for PQT12-3%NOBF4 and PQT12-5%PQTS12-3%NOBF4, respectively, in reasonable agreement with our measured Seebeck coefficients (Figure 2b) when divided by 320 K, the average temperature used for the E_A calculation. For T changing from 300 K to 345 K, an increase by a factor of 1.1, power factor only increases by a factor of 1.3. The plots also show what happens to power factor at constant E_F but variable T (Figure S13b). If T increases from 300 K (room temperature) to 375 K (about 100 ºC), an increase by a factor of 1.25, the calculated power factor only changes by about 10%. This indicates that the experimental test of the effect of changing T is in accordance with our model prediction of a small dependence.

Also, our results and theoretical calculations are in agreement with the concept proposed by Mahan and Sofo that the ideal position of the Fermi level is 2.4 k_BT (0.06 eV) (T = 300 K) away from the transport level.[50] Finally, the results also coincide with the power factor simulations of

Kemerink.[25] According to the calculations above, it is worth mentioning that, for two polymers with a preferred offset carrier energy level, the PF of the blend film can be best improved by higher mobilities with a prerequisite that two polymers and their blend film have analogous packing morphologies, which is confirmed by our results above.

3. Conclusions

We observed decoupling of the Seebeck coefficient and electrical conductivity by using alkylthio-substituted polymers as additives and two different dopants to delicately adjust the electrical structure of blend films. These two sets of polymers have similar structures and closely offset energy levels so that the morphology and mobility were not damaged after blending. Our results show that the trap states in blend films dominate the transport of carriers and affect the shift of the Fermi levels of blend films. Calculations and simulations of E_F - E_T for maximizing the power factor agree well with our result that closely offset HOMO levels of the two polymers are responsible for the increase of power factors in blend films. This work will give insights into how to further improve the power factor by choosing proper polymers and dopants for blends, especially by using pairs of higher mobility polymers where the molecular structures of the two polymers are homologous.

4. Experimental Section

Thermoelectric Device Fabrication and Characterization: Glass substrates (Corning Inc.) were cleaned by sonication in deionized water, acetone and *i*-propanol. Gold electrodes (50 nm thick) were deposited on glass with a channel length of 3 mm and a channel width of 6 mm. Polymer (5mg/mL) and F4TCNQ were dissolved (2 mg/mL) and stirred in hot chlorobenzene for 1 h, respectively. NOBF4 (5 mg/mL) was dissolved in tetrahydrofuran. Then, two polymer solutions were mixed with different weight ratios. All percentages mentioned in paper are mass percentage. After sonication for 30 min, F4TCNQ or NOBF4 was added into mixture and the mixed solution was sonicated for another 10 min. Finally, the resulting mixture was drop casted onto glass substrate on which 2D wells are fabricated by laying a pattern of Novec polymer. The thin films were dried in glovebox at 60 ºC for 30 min to remove residue solvent. All the measurements were performed in ambient (298 K). Resistance was measured by using four-probe measurement method with an Agilent 4155C Semiconductor Parameter Analyzer. At least

four measurements of resistance were performed on each sample surface in different positions. Seebeck coefficient can be calculated by S=ΔV/ΔT. Six ΔT values were imposed on the sample, so the slopes of ΔV versus ΔT give values of the Seebeck coefficient. Temperature-dependent measurements were conducted using the ZEM-5 TF Seebeck Coefficient/Electrical Resistance Measurement System (Advance Riko) under inert (He) atmosphere, starting from slightly above ambient temperature (310 K), conditions that lead to slightly higher conductivities than in ambient. Three values of ΔT were imposed on every temperature gradient.

OFET Fabrication and Characterization: Top contact/bottom gate OFET devices were fabricated. Highly n doped Si/SiO_2 substrates were cleaned and modified with hexamethyldisilazane (HMDS) self-assembled monolayer. The thin films were prepared by spin coating the solution on the substrates. Then the thin-film was annealed in vacuum oven to remove residue solvent. Gold contacts of 50 nm were deposited on the thin film as source and drain electrodes. The electrical performance of transistors was carried out using an Agilent 4155C Semiconductor Parameter analyzer in ambient. The mobility of films without doping was calculated in the saturation regime according to the equation: $I_{DS} = (W/2L)\mu C_i(V_G - V_T)^2$, where I_{DS} is the drain current, μ is the mobility, and V_G and V_T are the gate voltage and threshold voltage, respectively.

GIXRS measurements: GIXRS were obtained at the Advanced Photon Source (APS), Argonne National Laboratory using x-rays with a wavelength of λ = 1.6868 Å. The samples were prepared by drop casting the solution onto silicon wafer substrates.

Supporting Information. Supporting Information is available from the Wiley Online Library or from the author.

Acknowledgements

The GIXRS measurements were performed at Advanced Photon Source (APS) at the Argonne National Laboratory. We thank Zehua Zhao for helpful discussion about mathematic equations and simulation; and Professor Shannon Yee (Georgia Tech) and his student Shawn Gregory for

helpful insight about transport energy definitions. We are grateful to the National Science Foundation, Division of Chemistry, grant number 1708245, for funding the PBTTT(S)C12 synthesis, spectroscopy, and structural study. We thank the U.S. Department of Energy, Office of Science, Office of Basic Energy Sciences, under Award Number DEFG02-07ER46465, for support of the PQT(S)12 synthesis, thermoelectric measurements, electrochemistry, and theoretical analysis. We thank CAS Pioneer Hundred Talents Programme for support of the additional PQTS12 synthesis and temperature-dependent measurement.

References

[1] M. Chabinyc, *Nat. Mater.* **2014,** *13*, 119.

[2] R. Kroon, D. A. Mengistie, D. Kiefer, J. Hynynen, J. D. Ryan, L. Yu, C. Muller, *Chem. Soc. Rev.* **2016**, *45*, 6147.

[3] T. O. Poehler, H. E. Katz, *Energy & Environ. Sci.* **2012,** *5*, 8110.

[4] K. Shi, F. Zhang, C.-A. Di, T.-W. Yan, Y. Zou, X. Zhou, D. Zhu, J.-Y. Wang, J. Pei, *J. Am. Chem. Soc.* **2015,** *137*, 6979.

[5] X. Zhao, D. Madan, Y. Cheng, J. Zhou, H. Li, S. M. Thon, A. E. Bragg, M. E. DeCoster, P. E. Hopkins, H. E. Katz, *Adv. Mater.* **2017**, *139*, 1606928.

[6] B. Russ, A. Glaudell, J. J. Urban, M. L. Chabinyc, R. A. Segalman, *Nat. Rev. Mater.* **2016,** *1*, 16050.

[7] S. A. Gregory, A. K. Menon, S. Ye, D. S. Seferos, J. R. Reynolds, S. K. Yee, *Adv. Energy Mater.* **2018**, *8*, 1802419.

[8] H. Fritzsche, *Solid State Commun.* **1971,** *9*, 1813.

[9] D.-K. Ko, C. B. Murray, *ACS Nano* **2011,** *5*, 4810.

[10] Y. Sajad, P. Michael Thompson, *Nanotechnology* **2018,** *29*, 432001.

[11] S. D. Baranovskii, T. Faber, F. Hensel, P. Thomas, *J. Phys. Condens. Matter* **1997,** *9*, 2699.

[12] V. I. Arkhipov, E. V. Emelianova, G. J. Adriaenssens, *Phys. Rev. B* **2001,** *64*, 125125.

[13] O. Rubel, S. D. Baranovskii, P. Thomas, S. Yamasaki, *Phys. Rev. B* **2004,** *69*, 014206.

[14] G. Kim, K. P. Pipe, *Phys. Rev. B* **2012,** *86*, 085208.

[15] S. Ihnatsenka, X. Crispin, I. V. Zozoulenko, *Phys. Rev. B* **2015,** *92*, 035201.

[16] S. Dongmin Kang, G. Jeffrey Snyder, *Nat. Mater.* **2017**, *16*, 252.

[17] Y. Zou, D. Huang, Q. Meng, C.-a. Di, D. Zhu, *Organic Electron.* **2018**, *56*, 125.

[18] S. Krause, M. B. Casu, A. Schöll, E. Umbach, *New J. Phys.* **2008,** *10*, 085001.

[19] N. Lu, L. Li, M. Liu, *Phys. Chem. Chem. Phys.* **2016,** *18*, 19503.

[20] R. Schmechel, *J. Appl. Phys.* **2003**, *93*, 4653.

[21] J. Liu, L. Qiu, G. Portale, M. Koopmans, G. ten Brink, J. C. Hummelen, L. J. A. Koster, *Adv. Mater.* **2018**, *29*, 1701641.

[22] Z. Li, C. Xiao, S. Fan, Y. Deng, W. Zhang, B. Ye, Y. Xie, *J. Am. Chem. Soc.* **2015,** *137*, 6587.

[23] C. Xiao, Z. Li, K. Li, P. Huang, Y. Xie, *Acc. Chem. Res.* **2014,** *47*, 1287.

[24] J. Sun, M. L. Yeh, B. J. Jung, B. Zhang, J. Feser, A. Majumdar, H. E. Katz, *Macromolecules* **2010,** *43*, 2897.

[25] G. Zuo, X. Liu, M. Fahlman, M. Kemerink, *Adv. Funct. Mater.* **2018**, *28*, 1703280.

[26] G. Zuo, Z. Li, E. Wang, M. Kemerink, *Adv. Electron. Mater.* **2018,** *4*, 1700501.

[27] H. Li, J. Dailey, T. Kale, K. Besar, K. Koehler, H. E. Katz, *ACS Appl. Mater. Interfaces* **2017,** *9*, 20501.

[28] H. Li, M. E. DeCoster, R. M. Ireland, J. Song, P. E. Hopkins, H. E. Katz, *J. Am. Chem. Soc.* **2017**, *139*, 11149.

[29] E. Lim, K. A. Peterson, G. M. Su, M. L. Chabinyc, *Chem. Mater.* **2018**, *30*, 998.

[30] J. E. Cochran, M. J. N. Junk, A. M. Glaudell, P. L. Miller, J. S. Cowart, M. F. Toney, C. J. Hawker, B. F. Chmelka, M. L. Chabinyc, *Macromolecules* **2014,** *47*, 6836.

[31] D. T. Duong, C. Wang, E. Antono, M. F. Toney, A. Salleo, *Org. Electron.* **2013,** *14*, 1330.

[32] A. M. Glaudell, J. E. Cochran, S. N. Patel, M. L. Chabinyc, *Adv. Energy Mater.* **2015,** *5*,1401072.

[33] I. McCulloch, M. Heeney, C. Bailey, K. Genevicius, I. MacDonald, M. Shkunov, D. Sparrowe, S. Tierney, R. Wagner, W. Zhang, M. L. Chabinyc, R. J. Kline, M. D. McGehee, M. F. Toney, *Nat. Mater.* **2006,** *5*, 328.

[34] C. P. Jarrett, R. H. Friend, A. R. Brown, D. M. de Leeuw, *J. Appl. Phys.* **1995,** *77*, 6289.

[35] A. R. Brown, D. M. de Leeuw, E. E. Havinga, A. Pomp, *Synthetic Met.* **1994,** *68*, 65.

[36] E. M. Thomas, B. C. Popere, H. Fang, M. L. Chabinyc, R. A. Segalman, *Chem. Mater.* **2018**, *30*, 2965.

[37] M. L. Tietze, P. Pahner, K. Schmidt, K. Leo, B. Lüssem, *Adv. Funct. Mater.* **2015,** *25*, 2701.

[38] M. L. Tietze, L. Burtone, M. Riede, B. Lüssem, K. Leo, *Phys. Rev. B* **2012,** *86*, 035320.

[39] W. L. Kalb, S. Haas, C. Krellner, T. Mathis, B. Batlogg, *Phys. Rev. B* **2010,** *81*, 155315.

[40] N. Lu, L. Li, M. Liu, *Phys. Rev. B* **2015,** *91*, 195205.

[41] M. Ullah, I. I. Fishchuk, A. Kadashchuk, P. Stadler, A. Pivrikas, C. Simbrunner, V. N. Poroshin, N. S. Sariciftci, H. Sitter, *Appl. Phys. Lett.* **2010,** *96*, 213306.

[42] D. Venkateshvaran, M. Nikolka, A. Sadhanala, V. Lemaur, M. Zelazny, M. Kepa, M. Hurhangee, A. J. Kronemeijer, V. Pecunia, I. Nasrallah, I. Romanov, K. Broch, I. McCulloch, D. Emin, Y. Olivier, J. Cornil, D. Beljonne, H. Sirringhaus, *Nature* **2014**, *515*, 384.

[43] M. Cutler, N. F. Mott, *Phys. Rev.* **1969,** *181*, 1336.

[44] G. Zuo, H. Abdalla, M. Kemerink, *Phys. Rev. B* **2016,** *93*, 235203.

[45] N. F. Mott, E. A. Davis, Electronic Processes in Non-Crystalline Materials (2nd Edition) Oxford: 2012

[46] T. Menke, D. Ray, J. Meiss, K. Leo, M. Riede, *Appl. Phys. Lett.* **2012**, *100*, 093304.

[47] C.-Y. Yang, W.-L. Jin, J. Wang, Y.-F. Ding, S. Nong, K. Shi, Y. Lu, Y.-Z. Dai, F.-D. Zhuang, T. Lei, C.-A. Di, D. Zhu, J.-Y. Wang, J. Pei, *Adv. Mater.* **2018**, *30*, 1802850.

[48] K. Väkiparta, J. Moulton, A. J. Heeger, P. Smith, H. Isotalo, H. Stubb, *Synthetic Met.* **1991**, *41*, 903.

[49] M. T. Loponen, T. Taka, J. Laakso, K. Väkiparta, K. Suuronen, P. Valkeinen, J. E. Österholm, *Synthetic Met.* **1991**, *41*, 479.

[50] G. D. Mahan, J. O. Sofo, *P. Natl. Acad. Sci. USA* **1996,** *93*, 7436.

The table of contents entry:

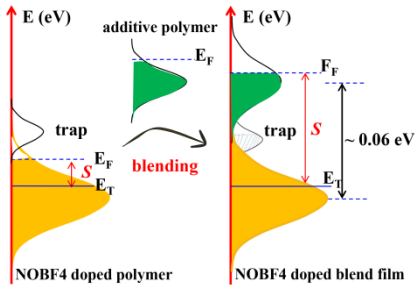

Decoupling of the Seebeck coefficient and electrical conductivity was achieved by blending pairs of polymers. Calculations and simulations for high power factor agree well with the idea that very closely offset carrier energy levels (~ 0.06 eV) of the two polymers are responsible for the increased power factors in blend films.